# CROSS-PROPERTY CONNECTION BETWEEN HEAT AND FORCE NETWORKS IN THERMALLY-ASSISTED COMPACTION OF GRANULAR MATERIALS

**Gülşad Küçük**[1], **Marcial Gonzalez**[2] **and Alberto M. Cuitiño** [3]

[1]Department of Mechanical and Aerospace Engineering, Rutgers University,
Piscataway, NJ, 08854, USA,
gulsad@gmail.com

[2]School of Mechanical Engineering Purdue University 585 Purdue Mall
West Lafayette, IN 47907-2088,
marcialgonzalez@purdue.edu

[3]Department of Mechanical and Aerospace Engineering, Rutgers University,
Piscataway, NJ, 08854, USA,
cuitino@jove.rutgers.edu

**Key words:** *thermo-mechanical coupling, heat networks, force networks, cross-property relation, granular materials, contact mechanics, thermally-assisted compaction*

Unlike the continuum media, granular materials host inhomogeneous distribution of contact networks, which results in uneven distribution of loads in the dense particulate assemblies. These structural arrangements play a critical role in determining the preferred paths of heat transport, due to the fact that thermal contact conductance is a function of normal force between the particles. In spite of the recent experimental and theoretical studies on the evolution of force chains, the formation of heat chains and the correlation between theses two networks still remain unclear. In this regard, a two dimensional discrete model based on particle mechanics approach is developed to unveil the short and large range relations of these networks' formation, and the effect of thermo-mechanical coupling on cross-property connection. Understanding the evolution of heat and force chains, and their influence on hot zone relations in the formation of these networks, represents a fundamental goal of granular mechanics, in terms of optimizing their collective behavior on macroscopic material properties.

For a particular loading condition that is mostly used in conventional engineering applications, numerical simulations are demonstrated to unveil some of the fundamental concepts in thermally-assisted compaction of granular materials. These are: (i) formation of force and heat chains (ii) alterations in force and heat distributions with respect to compaction parameters, (iii) cross-property relation between normal force and heat transferred at the contact surfaces.

## 1 Introduction

Understanding the fundamental multi-physics behind the thermo-mechanically coupled deformation of granular systems and its projections in macroscopic scale provides the essentials to fabricate particulate assemblies with specific functionalities. A proper estimate of the mechanical strength, thermal and electrical conductivity of a compacted solid is contingent upon the knowledge of microstructure formation during the deformation stage of the compression. In this regard, current study looks at unveiling the cross-property connection between the two dominant mechanisms that determine the overall mechanical and transport properties of the consolidated material.

Experimental studies on static and dynamic granular systems reveal a highly heterogeneous distribution of force network formation, which is impossible to observe in a solid, liquid or gas (Jaeger et al. 1996). Visualization of interparticle forces in a granular media by photoelastic or carbon paper techniques shows that special structural arrangements arose to serve the purpose of supporting most of the external load, while leaving the other particles unloaded or less loaded (Majmudar & Behringer 2005, Mueth et al. 1998, Blair et al. 2001, Løvoll et al. 1999, Snoeijer et al. 2004). The force chains can be treated as the load bridges, which usually stand several times larger forces than the rest of the system (Antony 2007). In static silos these mechanisms are responsible for enhancing arch formations and in dynamic loading cases altering deformation patterns. It has been also argued that uneven distribution of force chains cause localized fracture and hot spot formations where the process may trigger chemical wave front propagation or phase transition, due to the instant change of temperature or redundant contact forces (Foster Jr et al. 2002).

More recently, a study on packing grains by thermal cycling elucidated the collective behavior of particulate materials and became an inspiration for various engineering applications. Chen and his co-workers investigated the influence of thermal cycling on packing fraction by examining a loosely packed bed of glass beads in a plastic container (Chen et al. 2006). The difference in thermal expansion property of the beads and the container is shown to have a critical effect on beads re-arrangement, which is similar to mechanical agitation on altering grain packing (Chen et al. 2006). It is also proved that arch formations within the granular assemblies lead up to giant stress fluctuations that are mostly associated with the extreme sensitivity of stress paths to small perturbations, such as; applied thermal gradient on the granular system (Liu & Nagel 1992, Claudin & Bouchaud 1997).

Due to the fact that traditional material examination methods, which mostly rely on post process characterization, provide very poor or inaccurate information in the prospect of revealing the driving mechanisms, there exists an inevitable need for simulations based on detailed micro level information. In this regard two major approaches have been adopted to unveil the formation of force distributions within granular assemblies. These approaches differ by how they define the initial problem, which are a continuum media and a discrete system of particles. The well-known paper in the former group is a stochastic model, named as 'q-model', that explains the probability distribution of contact forces in bead packs by using statistical mechanics (Liu et al. 1995). Also being proved by experimental studies, this model suggests that normal contact force distribution obeys a decaying exponential law for the forces that are above the average (Liu et al. 1995, Coppersmith et al. 1996, Claudin & Bouchaud 1997). The latter approach works on particle interactions and the constitutive relations of contact mechanics. Discrete element methodology has been widely used in the field of particle scale research (Zhu et al. 2007). The early work of Cundall and Strack on granular dynamics is based on an explicit numerical scheme, through which the particles interactions are calculated over the contact networks and particle motion is determined by the state of force balance equilibrium (Cundall & Strack 1979). This technique is adopted by many engineering fields to analyze the dynamic, quasi-static and static stress-strain behavior of an assemble of distinct objects (Makse et al. 2000, Radjai & Roux 1995, Radjai et al. 1996).

The problem of thermally-assisted compaction entails the integration of contact mechanics principles with thermal-contact model analytical solutions to account for the effective modeling of heat conduction within the deformed state of granular materials. In this regard Vargas and McCarthy introduced a thermal particle dynamics model, by which they track the formation of stress and heat front during thermally-assisted compaction of binary size particles (Vargas & McCarthy 2001). They showed that similar to stress chains; there exists preferable paths to conduct heat within the granular bed, which are recalled as heat chains. Surprisingly stress chains and heat chains are not identical, however they share the same characteristic of being unevenly distributed and being dependent on the loading conditions (Vargas & McCarthy 2001, 2007). Feng et al. extended the numerical methodology used in discrete element modeling for systems comprising a large number of circular particles in 2D cases (Feng et al. 2008). Starting from the analytical integral solution for the temperature distribution over a circular body, system of thermal conductivity equations is derived in terms of the average temperatures and the resultant fluxes at the contact zones with the neighboring particles (Feng et al. 2008). Unlike the finite element method, discrete mechanics provide a very reasonable solution accuracy, where it has also no discretization errors involved in the numerical assessments (Feng et al. 2008). Even though there still exists computational challenges in carrying out calculations on a large number of particles, which undergoes highly nonlinear system of coupled deformations, in this research we work on advances in numerical methods to enhance the feasibility and efficiency of computational mechanics.

It is the purpose of this study to provide that insight into the nature of thermo-mechanical interactions, that determine the microstructure formation of the thermally-assisted compaction of granular assemblies. We consider a packed two dimensional arrangement of spherical particles compressed by heated boundary walls. We introduce a particle mechanics approach to simulate multi-body system characteristics of granular beds starting from the pair interactions of particles defined by thermo-elastic contact models. We trace the evaluation of contact networks at each quasi-static equilibrium state and address the intriguing question of how the force chains are related to heat chains.

## 2 Particle Mechanics Approach

Our point of departure for the discrete model is to integrate the well-known theory of Hertzian deformation for quasi-static mechanics and conductive heat transfer for spherical conforming contacts of granular media.

We present a multi-body system model of granular beds starting from the pair interactions of particles defined by thermo-elastic contact models. This concept is similar to recent studies of Vargas & McCarthy (2001), and Vargas & McCarthy (2007), where they introduce a mathematical model as an extension to the discrete element model of granular materials. However, our approach is based on defining particles' final state, such as position and temperature, rather than tracking particles during the compaction process. Details of the approach adopted in this study can be also found in our earlier work (Küçük et al. 2015).

The following nomenclature is used in integration of thermal and mechanical deformation models.

Table 1: Nomenclature

| | |
|---|---|
| $R^m$ | Radius of the individual particle m |
| $T^m$ | Temperature of the particle m |
| $\alpha^m$ | Thermal expansion coefficient of particle m |
| $E^m$ | Young Modulus of the particle m |
| $\nu^m$ | Poisson's ratio of the particle m |
| $k^m$ | Thermal conductivity of the solid particle m |
| $H^{mn}$ | Thermal contact conductance at that contact of particles m and n |
| $a^{mn}$ | Radius of contact area at the mutual interface of particles m and n |
| $\gamma^{mn}$ | Overlap at the contact of particles m and n |
| $T^{wall}$ | Temperature of the wall |
| $Tws$ | Temperature at the wall surface, in contact with the boundary particle |
| $h^w$ | Convective heat transfer coefficient of the wall |

The temperature and the position of particles are obtained through the equilibrium for the system particles. The total heat transferred to particle m from neighboring particles n and the total of forces acting on particle m are equated to zero.

$$Q^m = \sum_{n \epsilon \mathcal{N}_m} Q^{mn} = 0 \tag{1}$$

$$\mathbf{F}^m = \sum_{n \epsilon \mathcal{N}_m} F^{mn} \mathbf{n}^{mn} = 0 \tag{2}$$

where $\mathbf{n}^{mn}$ is the unit normal vector defined from centers of particle n to particle m.

$$\mathbf{n}^{mn} = \frac{\mathbf{x}^m - \mathbf{x}^n}{\|\mathbf{x}^m - \mathbf{x}^n\|} \tag{3}$$

Small-strain elasticity of granular media are determined from contact mechanics considerations (Johnson 1987). These relations define the deformation of locally spherical, elastic particles that are subject to a compression load. Slight deformation of conforming surfaces results in a flat circle of contact area whose dimensions are formulated through Hertz theory (Landau & Lifshitz 1959). Collinear contact force for elastic contact of two smooth spherical particles m-n is defined through Young's modulus, $E^m$ and $E^n$; Poisson's ratio, $\nu^m$ and $\nu^n$; particle radii, $R^m$ and $R^n$; and overlap $\gamma^{mn}$ that occurs along the contact line.

$$F^{mn} = \frac{4}{3} E^{mn} (R^{mn})^{1/2} (\gamma^{mn})^{3/2} \tag{4}$$

where

$$R^{mn} = \left[ \frac{1}{R^m} + \frac{1}{R^n} \right]^{-1} \tag{5}$$

$$E^{mn} = \left[ \frac{1-(\nu^m)^2}{E_m} + \frac{1-(\nu^n)^2}{E_n} \right]^{-1} \tag{6}$$

$$\gamma^{mn} = R^m + R^n - \|\mathbf{x}^m - \mathbf{x}^n\| \tag{7}$$

In this study we investigate the effect of thermal expansion on the steady state equilibrium of thermal and mechanical loading conditions. While the temperature and position of each particle is being tracked for any particular loading condition, the particle radius, $R^m$, is evaluated at the specified temperature $T^m$, thereby making the active radius $R^{mn}$ temperature dependent.

$$R^m = R^m_{ref} \left[ 1 + \alpha^m \left( T^m - T^m_{ref} \right) \right] \tag{8}$$

where $\alpha^m$ is the thermal expansion coefficient, $T_{ref}$ is the reference temperature and $R^m_{ref}$ is the radius of particle at the reference temperature.

Due to the dependence of contact geometry on thermo-mechanical coupling imposed by the defined problem, it is expected to capture a distribution of contact area formation throughout the compacted medium.

There has been considerable research on modeling the thermal-contact of deformed bodies. The major heat transfer mechanisms are: conduction through solid, conduction through the contact area between two touching particles, conduction to/from interstitial fluid, heat transfer via convection, radiation between particle surfaces, radiation between neighboring voids (Vargas & McCarthy 2001). Under the prescribed thermally-assisted compaction conditions in this study, the first two of the above are assumed to be the main contributors in heat transfer through the particulate bed.

The problem of heat transfer regarding the compaction of particles, which are in or nearly in contact, is deeply investigated by a number researchers (Chan & Tien 1973, Kaganer 1966, Batchelor & O'Brien 1977). In this study we adopt Batchelor and O'Brien's thermal-contact model. In an attempt to find the approximate effective thermal conductivity of ordered and randomly packed granular beds, Batchelor and O'Brien states the heat flux across the flat circle of contact between smooth, conforming, and elastic particles.

$$Q^{mn} = H^{mn}(T^m - T^n) \tag{9}$$
$$H^{mn} = 2a^{mn}k^{mn} \tag{10}$$

$H^{mn}$ is contact conductance, which defines the ability of two conforming particles to transmit heat across their mutual interface. $k^{mn}$ is the arithmetic mean of the thermal conductivities of two particles in contact, and $a^{mn}$ is the Hertzian contact area.

$$k^{mn} = \frac{1}{2}\left[\frac{1}{k^m} + \frac{1}{k^n}\right]^{-1} \tag{11}$$
$$a^{mn} = \sqrt{\gamma^{mn}R^{mn}} \tag{12}$$

The total heat flow to an individual particle (equation 1) is calculated by adding the heat flow at each contact of the particle between its neighboring particles (equation 9). In the current study, we assume that the temperature at each contact of an individual particle is equal to the temperature calculated at the center of the particle. In other words the temperature does not very significantly within the particle, which also imposes that the contact conductance alone the mutual interface of conforming particles is relatively smaller than the heat conductance within the particle.

$$\frac{2k^{mn}a^{mn}}{k^{mn}A/R^m} << 1 \tag{13}$$

where A is the cross sectional area, $\pi(R^m)^2$. In other words expression given in equation 13 defines the state of Biot number much less than 1. This assertion is applied by several authors in earlier studies (Vargas & McCarthy 2001, Siu & Lee 2004). The condition of $a^{mn} << R^{mn}$ is also required by the contact mechanics model.

### 2.1 Methodology

Random packing of particles is generated by using ballistic deposition technique, which is developed by Gioia et al. (2002). Based on the gradually applied thermal and mechanical boundary conditions, inter-particle and wall-particle interactions are estimated. Starting from an initial guess for the position and temperature of the particles, system of nonlinear equations that define the force and heat transfer at each particle are solved at quasi-static mechanical and steady state thermal equilibrium. Newton-Raphson method is implemented in the direct iterative solution. Rigid wall assumptions are used in evaluating the state of boundary particles, which are in contact with walls. Analogous to ghost-cell method, boundary particle-adjacent wall interaction is simulated as the contact between a particle and a ghost particle, where both are symmetrically deformed. Ghost particle is assumed to have the same material properties and radius with the boundary particle.

The boundary wall is assumed to be located in the midst of these symmetrically deformed particles. The temperature difference between the ghost particle and the wall surface is the same as the temperature difference between the wall surface and the boundary particle.

## 2.2 Simulation Configuration

In the two dimensional numerical experiments the particles are shown as circles, and the boundary walls are presented with solid lines. Initially the particles are assumed to be at point contact, upon the application of thermal and mechanical loads the particles change place and settle down while reaching a steady state temperature to adjust with the overall temperature gradient of the system. Incremental deformations are applied in a quasi-static manner, beginning with a stress-free state. In order to avoid the dominant influence of boundaries and to minimize the local fluctuations of spatially dependent properties, we focus on a particulate system, which is a few tens of particles diameters. This concept has been agreed to provide statistical homogeneity by Radjai et al. (1996) and verified by previous experimental studies of Rothenburg & Bathurst (1989), Emeriault & Cambou (1996).

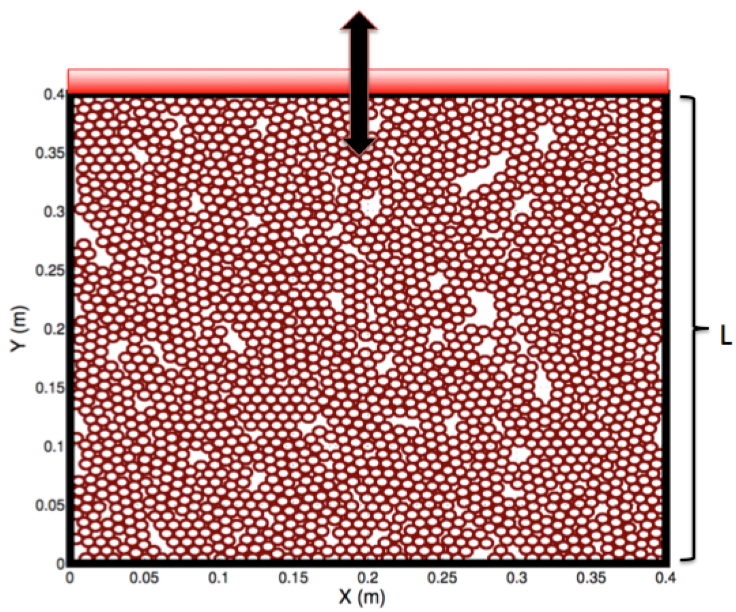


Figure 1: Undeformed configuration of a 2077 particles system. Initial length in the $x$ and $y$ direction is 0.4 m.

As shown in figure 1 initial configuration is a randomly arranged bed of 2077 stainless steel particles with Young's modulus, $E$, 193 GPa; thermal conductivity, $k$, 15 $\mathrm{W/mK}$; Poisson's ratio, $\nu$, 0.29; thermal expansion, $\alpha$, 17.3 $10^{-6}$ $1/\mathrm{K}$. The particles of 4 mm in radius are contained in a bed of 0.4 m in width and height, $L$. Compression along the $yy$ direction is created by the incremental downward movement of the top wall, which acts a punch. The other three walls are fixed and kept at reference temperature. The total strain, $\epsilon_{yy} = |\Delta L/L|$, applied on the system is equal to the compaction ratio. In order to consider the effect of temperature increase and thermal expansion, thermal gradient is induced through the top heated wall and the particles in touch with this boundary. The packing density of the undeformed system of particles is 0.72. The weight of the particles is neglected in two-dimensional analysis.

## 3 Fundamental Concepts in 2D Discrete Modeling of Granular Materials

Based on the proposed particle mechanics approach, we conduct numerical analysis to exploit the dependence of the contact network with regard to the formation of force and heat chains within the confined granular bed. We investigate the normal contact force and heat distributions in the prospect of understanding the cross-property connection between force and heat distributions.

### 3.1 Force Chains

Force chains that form the skeleton of compacted granular materials (Ostojic et al. 2006), can be visualized by representing normal forces at contacts as bonds between the conforming particles. The thickness of line segment connecting the particles is proportional to the magnitude of the normal contact force that is above the average. In force and heat chain representations, we plot the particles as circles filled with black color, and surrounded by a red line. The force chains are shown as blue lines. To provide o more trackable visualization we prefer to show the heat gradient within the particulate bed, by altering the color filling of each particle. In the following figures the filling color of circles is changed from black to red, as the temperature of particles increases.

For a system of 2077 stainless steel particles, initially we consider two cases of compaction. In both cases mechanical deformation is imposed gradually by moving the top wall. The total deformation is $\epsilon_{yy} = 0.08$. In the first case the boundary walls are kept at reference temperature of 293 K, whereas in the second case only the top wall is elevated to a higher temperature of 493 K while keeping the other three walls at 293 K. The formation of force chains in the former case, which is a purely mechanical deformation, is plotted in figure 2a.

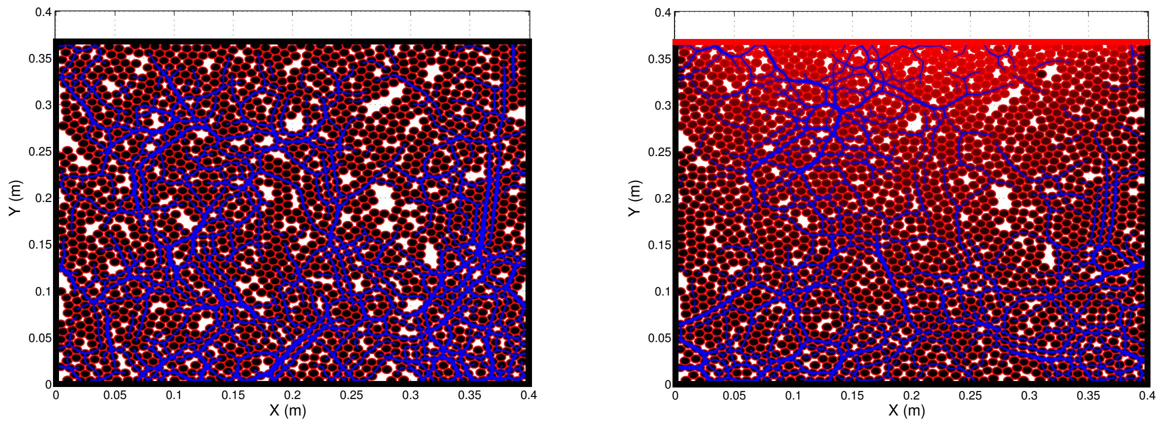


(a) Particle system under the sole of effect of mechanical deformation.

(b) Particle system under the coupled field of thermal and mechanical deformation. $T_{punch}$ = 493 K.

Figure 2: Force chains developed in compaction of 2077 stainless steel particles' system. Compaction strain, $\epsilon_{yy} = 0.08$.

In figure 2b the thickness of the line segments are seen to be relatively decreased, and the intensity of horizontal force chains are increased. It is also observed that thermal gradient is inducing larger contact forces around the heated punch.

### 3.2 Heat Chains

During the process of thermally-assisted compaction, the confined granular bed is under the effect of a thermal gradient, which triggers a formation of preferred paths of heat transport within the assembly. In order to visualize the heat chains, we use a similar approach as in evaluation of force chains. The heat transferred at each contact is mapped into the contact network, shown in lines whose thickness is proportional to the heat flux. In figure 3, we represent the heat chains developed in the system of 2077 randomly packed particles that are compacted by a ratio of 8% and heated through the top wall, which is kept at 493 K.

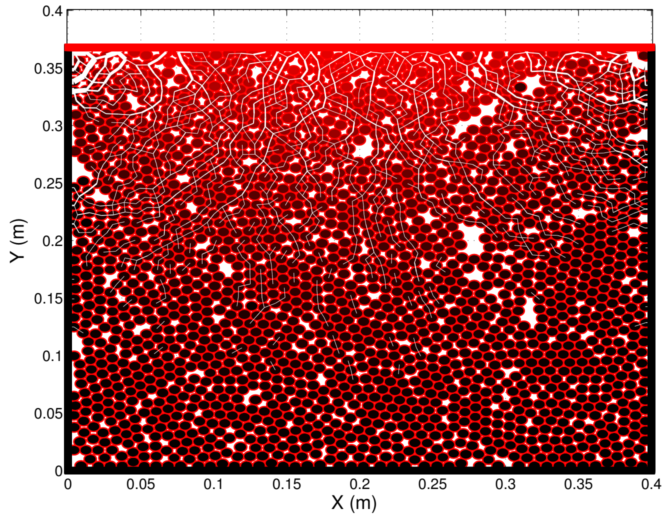


Figure 3: Heat chains developed in thermally-assisted compaction of 2077 stainless steel particles system. Punch temperature is kept at 493 K. The total mechanical deformation is $\epsilon_{yy} = |\Delta L/L| = 0.08$.

Unlike the force network, the heat chains are accumulated closely to the boundary at the elevated temperature. Although heat conductance is a function of the contact area between the conforming surfaces, figure 3 shows that the preferred paths of heat transfer depends strongly on the spatial orientation of applied thermal gradient on the particulate bed.

### 3.3 Contact Force Distribution

A widely used characterization parameter to quantify the formation of force chains is the probability distribution of individual contact forces. There exists a broad spectrum of statistical mechanics studies (Liu et al. 1995, Coppersmith et al. 1996, Makse et al. 2000, Snoeijer et al. 2004) and experimental studies (Løvoll et al. 1999, Blair et al. 2001, Foster Jr et al. 2002, Majmudar & Behringer 2005) developed to estimate the probability of normal contact force distribution within static and consolidated granular materials. The force distributions are expressed in terms of non-dimensional variable, $f$, that defines the normal force at the contact divided by the average of these contact forces, $f = F/F_{ave}$. In a typical granular packing, the probability distribution, $P(f)$, has an exponentially decaying tail at $f > 1$, and a plateau at $f < 1$.

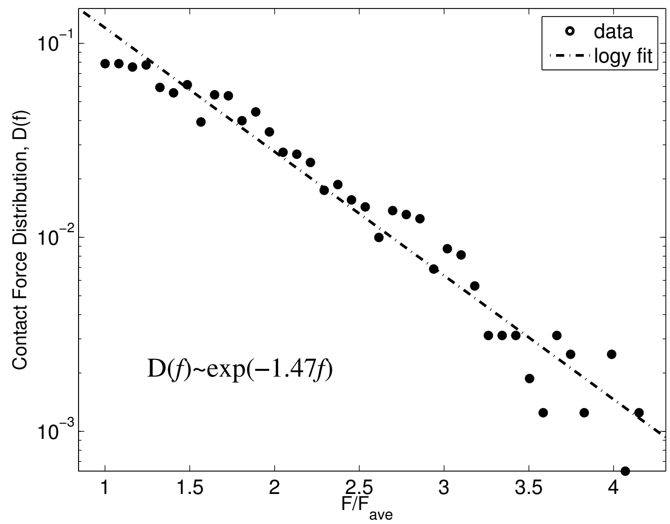


Figure 4: Normalized contact force distribution of athermally compacted 2077 stainless steel, SS304, particles system.

Based on our particle mechanics approach we trace the normal contact forces that are above the average, at each contact. In figure 4 we plot the distribution of normalized contact forces $f$ for the system of 2077 particles that is compressed by the downward movement of the top boundary. The total strain, $\epsilon_{yy} = \Delta L/L$, imposed on the system is 0.08, and no thermal gradient is applied. We estimate the normalized contact force distribution by an exponential decay function, which can be shown as:

$$D(f) \propto e^{\beta f}, \;\; f > 1 \tag{14}$$

where $\beta = -1.4722$.

We investigate the dependence of packing fraction on the contact force distribution. The system of 2077 particles is gradually compressed by lowering the top wall. The normalized force distributions of the contacts are evaluated at compaction rates, 2%, 4%, 6% and 8%.

In the absence of applied thermal gradient on the system, the normalized contact force distributions coincide over at the range of $\beta \approx -1.4 \pm 0.1$, as seen in figure 5. The off-range value obtained at $\epsilon_{yy} = 0.02$ is attributed to the loosely packed structure of contact network. In figure 6 the normalized contact force distributions are plotted when the top wall, the punch, is kept at a temperature of 493 K. Although the general trend of the distribution is the same, a remarkable change in the exponential power is experienced, $\beta^T \approx -0.85 \pm 0.25$.

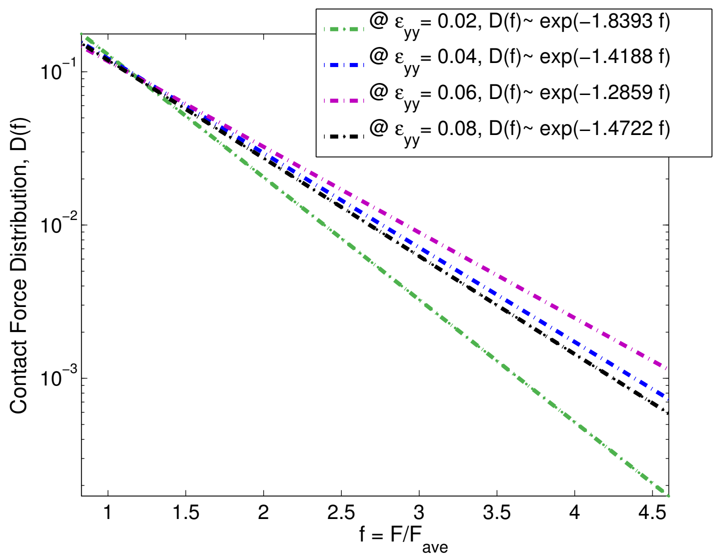


Figure 5: Comparison of force distributions for a gradually compacted system of 2077 particles. The total strain is $\epsilon_{yy} = |\Delta L/L| = 0.08$.

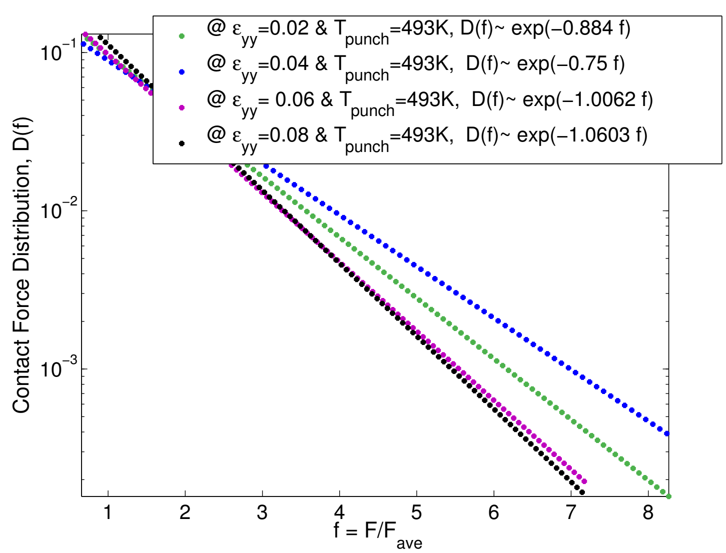


Figure 6: Comparison of force distributions for a gradually compacted system of 2077 particles. The total strain is $\epsilon_{yy} = |\Delta L/L| = 0.08$. Punch temperature is kept at 493 K.

### 3.4 Heat Distribution

Similar to force distribution analysis, we investigate the heat distribution within the contact network. The numerical simulations point out that the normalized heat distribution can be distinctly expressed in log-log plots. In figure 7 the heat distribution of 2077 particles system is shown for the particular loading of compaction ratio, $\epsilon_{yy} = 0.08$ and the top wall kept at 493 K.

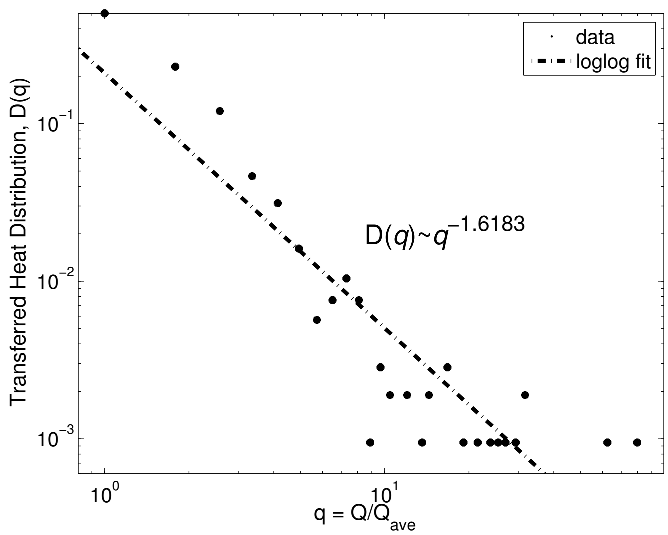


Figure 7: Normalized heat distribution of 2077 stainless steel particles' system $T_{punch} = 493K$ and the total strain, $\epsilon_{yy} = 0.08$.

$$D(q) \propto q^{\zeta}, \;\; Q > Q_{ave} \tag{15}$$

where $\zeta = -1.6183$. In order to understand the effect of applied thermal gradient on the heat distribution characteristics, the same system is investigated in a gradually heated numerical experiment. The particle assembly is compacted by a ratio of 8%, and the temperature of the top wall is increased from 293 K to 493 K, by increments of 40 K. Figure 8 summarizes that $D(q) \approx q^{-1.7\pm0.1}$ for the particular thermal gradient range.

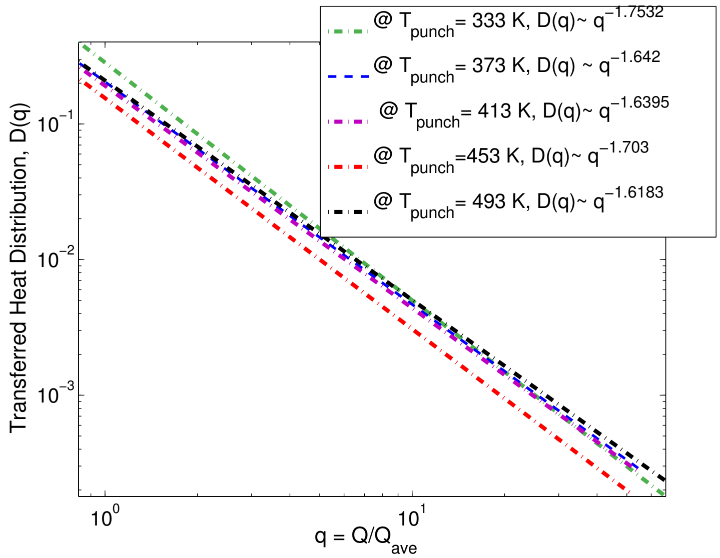


Figure 8: Comparison of heat distributions for a gradually heated system of 2077 particles, under effect of the total thermal gradient of 200 K, and the total strain, $\epsilon_{yy} = 0.08$.

### 3.5 Cross-Property Relation Between Force and Heat Distributions

In this study we aim to explain the role of heat transfer in contact force distribution and the role of the compaction ratio in heat transfer distribution within the particulate bed quantitatively. Figure 9 points out one of the unique characteristic of thermally-assisted compaction. The exponential power, which indicates distribution of contact forces above the mean, decreases up to 25 % of its initial value, as the applied thermal gradient on the system is increased. Although we observe the peak around the same mean, the system, which is in under a larger thermal load, has a much slower decaying exponential tail. It is a clear sign of a more uniform microstructure with less deep fluctuations in distribution of contact forces. Applied thermal gradient not only changes the particle re-arragement and packing density remarkably, as explained earlier in Chen et al. (2006), but also has a significant effect on the contact force distributions of the confined granular medium.

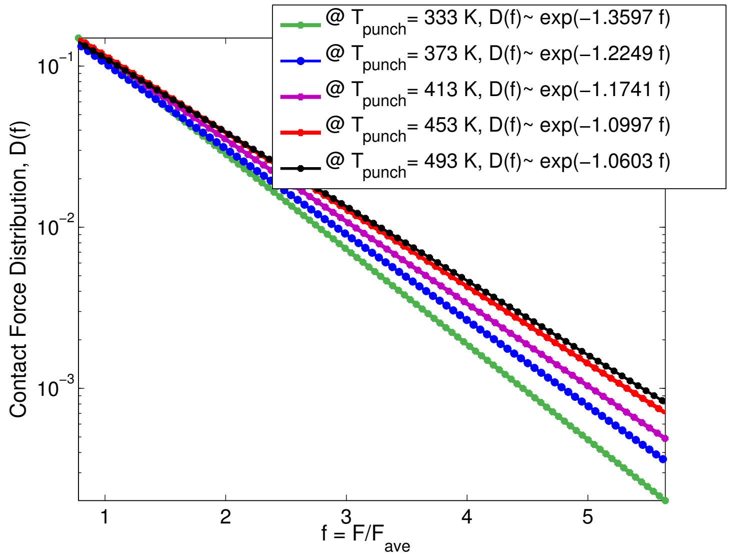


Figure 9: Comparison of force distributions under different thermal boundary conditions. System of 2077 stainless steel particles is compacted by a ratio of % 8, while the thermal gradient imposed between the top and bottom boundary walls is increased from 40 K to 200 K, gradually.

In figure 10 heat distributions of a gradually heated confined system of particles is traced. The correlation between heat distribution and compaction ratio reveals that the packing density plays a critical role in determining the steady state solution of the system. The power exponent, which characterizes the heat distribution, seems to converge the same value $\zeta^{\epsilon} \approx -1.7 \pm 0.1$, over a certain packing density. Although the formation of heat chains deviate significantly from the formations of force chains, the main mechanism that determine the overall heat distribution is dominantly controlled by the contact network formation.

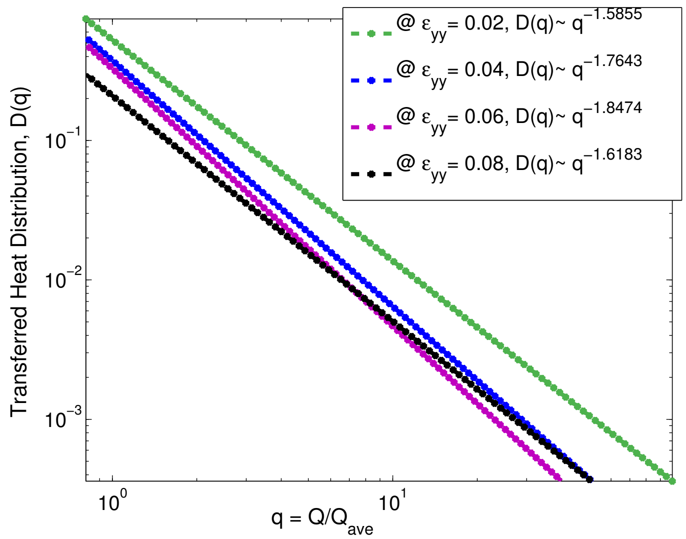


Figure 10: Comparison of heat distributions under different mechanical loading conditions. System of 2077 stainless steel particles is under the effect of a thermal gradient, 200 K, while it is compacted up a ratio of % 8, gradually.

In the view of these finding, we would like to underline a characteristic about the current experimental set-up. The exponential tail of the distribution of forces comprises nearly 40 % and power law decay of heat distribution constitutes around 30 % of all contacts. It is also important to notice that the extremely large values seen as rare sequence in normalized distributions of force and heat are corresponding to particle-boundary wall contacts. We suggest that, to obtain more accurate and predictive models at moderate levels of deformation and high confinement, Hertz law can be replaced by the nonlocal contact formulation (Gonzalez & Cuitiño 2012, 2015).

## 4 Conclusions

Particle scale modeling of thermally-assisted compaction requires extension of the discrete element method to account for the effective modeling of heat conduction, which indeed similar in spirit to understand and develop platforms for other widely encountered coupled phenomena such as; thermo-electrical, electro-mechanical processes. There exist two important contributions of the present work to the family of coupled problems. Former is to propose a particle mechanics approach that unveils the key characteristics of the thermally-assisted compaction in two dimensional numerical experiments for a system of large number of particles. Latter is to introduce this numerical platform to conduct numerical experiments in the light of understanding the cross-property connection between two dominant mechanisms that determine the macroscopic properties of the consolidated material.

Our methodology is capable of capturing the contact networks, force and heat chains within the granular bed. Despite the fact that these chains visually reveal the hot zone localizations and the potential arching spots, it is not feasible to trace the formation of them on microstructural scale, particularly for the case of systems with large number of particles. However the force and heat distributions provide significant insight about understanding the driving mechanisms in a quantitative manner.

Simulations show that force distribution of a densely packed spherical particles system is cumulated around an average normal contact force value, which is determined by the loading conditions, and material properties of the compacted sample. Above the average normal contact force value, this distribution tends to decay out obeying an exponential power law. The extremely large values of normal contact force can be used in estimation of potential of micro-crack in further analysis. Similar to contact force distribution analysis, we investigate the heat distributions and their correlation with the heat chains formations. Tracing the heat transferred at each inter-particle contact we conclude that heat distribution distribution obeys a general decaying power law. For the particular loading condition it is noticed that the normalized heat distribution is independent of the thermal gradient applied on the system.

In recognition of the ubiquity of thermally-assisted compaction problem, there is an inevitable need for granular material simulations to search for the cross property relation of the force and heat chain formation with respect to thermal gradient imposed on the system and compaction ratio. Our numerical results show that the thermo-mechanical coupling enhances the uneven distributions of force chains. The exponential decay seen in force distribution analysis is extended, revealing the fact that thermally-assisted compaction not only induces larger contact forces, but also the frequency to experience forces larger than average is increased. The correlation between heat distribution and compaction ratio reveals that the contact network formation becomes dominant in determining the heat distribution after a certain packing density is achieved.

## Acknowledgement

This work has been partially supported by U.S. Army ARDEC grant under the project titled as: Multifunctional Nanomaterials: Processing, Properties, and Applications.

## References

Antony, S. (2007), 'Link between single-particle properties and macroscopic properties in particulate assemblies: role of structures within structures', *Philosophical Transactions of the Royal Society A: Mathematical, Physical and Engineering Sciences* **365**(1861), 2879–2891.

Batchelor, G. & O'Brien, R. (1977), 'Thermal or electrical conduction through a granular material', *Proceedings of the Royal Society of London. A. Mathematical and Physical Sciences* **355**(1682), 313–333.

Blair, D. L., Mueggenburg, N. W., Marshall, A. H., Jaeger, H. M. & Nagel, S. R. (2001), 'Force distributions in three-dimensional granular assemblies: Effects of packing order and interparticle friction', *Physical Review E* **63**(4), 041304.

Chan, C. & Tien, C. (1973), 'Conductance of packed spheres in vacuum', *J. Heat Transfer;(United States)* **95**(3).

Chen, K., Cole, J., Conger, C., Draskovic, J., Lohr, M., Klein, K., Scheidemantel, T. & Schiffer, P. (2006), 'Granular materials: Packing grains by thermal cycling', *Nature* **442**(7100), 257–257.

Claudin, P. & Bouchaud, J.-P. (1997), 'Static avalanches and giant stress fluctuations in silos', *Physical review letters* **78**(2), 231.

Coppersmith, S., Liu, C.-h., Majumdar, S., Narayan, O. & Witten, T. (1996), 'Model for force fluctuations in bead packs', *Physical Review E* **53**(5), 4673.

Cundall, P. A. & Strack, O. D. (1979), 'A discrete numerical model for granular assemblies', *Geotechnique* **29**(1), 47–65.

Emeriault, F. & Cambou, B. (1996), 'Micromechanical modelling of anisotropic non-linear elasticity of granular medium', *International Journal of Solids and Structures* **33**(18), 2591–2607.

Feng, Y., Han, K., Li, C. & Owen, D. (2008), 'Discrete thermal element modelling of heat conduction in particle systems: Basic formulations', *Journal of Computational Physics* **227**(10), 5072–5089.

Foster Jr, J. C. et al. (2002), 'Dynamic stress chain formation in a two-dimensional particle bed', *Experimental mechanics* **42**(3), 329–337.

Gioia, G., Cuitiño, A. M., Zheng, S. & Uribe, T. (2002), 'Two-phase densification of cohesive granular aggregates', *Physical review letters* **88**(20), 204302.

Gonzalez, M. & Cuitiño, A. M. (2012), 'A nonlocal contact formulation for confined granular systems', *Journal of the Mechanics and Physics of Solids* **60**(2), 333–350.

Gonzalez, M. & Cuitiño, A. M. (2015), 'Microstructure evolution of compressible granular systems under large deformations', *Under review* .

Jaeger, H. M., Nagel, S. R. & Behringer, R. P. (1996), 'Granular solids, liquids, and gases', *Reviews of Modern Physics* **68**(4), 1259–1273.

Johnson, K. L. (1987), *Contact mechanics*, Cambridge university press.

Kaganer, M. (1966), 'Contact heat transfer in granular material under vacuum', *Journal of engineering physics* **11**(1), 19–22.

Küçük, G., Gonzalez, M. & Cuitino, A. M. (2015), 'Thermo-mechanical behavior of confined granular systems', *Lecture Notes in Applied and Computational Mechanics, Innovative numerical approaches for coupled multi-scale problems* .

Landau, L. & Lifshitz, E. (1959), *Theory of Elasticity*, Pergamon Press.

Liu, C.-h. & Nagel, S. R. (1992), 'Sound in sand', *Physical review letters* **68**(15), 2301.

Liu, C., Nagel, S. R., Schecter, D., Coppersmith, S., Majumdar, S., Narayan, O. & Witten, T. (1995), 'Force fluctuations in bead packs', *SCIENCE-NEW YORK THEN WASHINGTON-* pp. 513–513.

Løvoll, G., Måløy, K. J. & Flekkøy, E. G. (1999), 'Force measurements on static granular materials', *Physical Review E* **60**(5), 5872.

Majmudar, T. S. & Behringer, R. P. (2005), 'Contact force measurements and stress-induced anisotropy in granular materials', *Nature* **435**(7045), 1079–1082.

Makse, H. A., Johnson, D. L. & Schwartz, L. M. (2000), 'Packing of compressible granular materials', *Physical review letters* **84**(18), 4160–4163.

Mueth, D. M., Jaeger, H. M. & Nagel, S. R. (1998), 'Force distribution in a granular medium', *Physical Review E* **57**(3), 3164.

Ostojic, S., Somfai, E. & Nienhuis, B. (2006), 'Scale invariance and universality of force networks in static granular matter', *Nature* **439**(7078), 828–830.

Radjai, F., Jean, M., Moreau, J.-J. & Roux, S. (1996), 'Force distributions in dense two-dimensional granular systems', *Physical review letters* **77**(2), 274.

Radjai, F. & Roux, S. (1995), 'Friction-induced self-organization of a one-dimensional array of particles', *Physical Review E* **51**(6), 6177.

Rothenburg, L. & Bathurst, R. (1989), 'Analytical study of induced anisotropy in idealized granular materials', *Geotechnique* **39**(4), 601–614.

Siu, W. & Lee, S.-K. (2004), 'Transient temperature computation of spheres in three-dimensional random packings', *International journal of heat and mass transfer* **47**(5), 887–898.

Snoeijer, J. H., Vlugt, T. J., van Hecke, M. & van Saarloos, W. (2004), 'Force network ensemble: a new approach to static granular matter', *Physical review letters* **92**(5), 054302.

Vargas, W. L. & McCarthy, J. (2001), 'Heat conduction in granular materials', *AIChE Journal* **47**(5), 1052–1059.

Vargas, W. L. & McCarthy, J. (2007), 'Thermal expansion effects and heat conduction in granular materials', *Physical Review E* **76**(4), 041301.

Zhu, H., Zhou, Z., Yang, R. & Yu, A. (2007), 'Discrete particle simulation of particulate systems: theoretical developments', *Chemical Engineering Science* **62**(13), 3378–3396.